Influence of the Methylene Blue Dye (MBD) on the corrosion inhibition of mild steel in 0.5 M sulphuric acid, Part I: weight loss and electrochemical studies

Omar Benali [a*], Lahcene Larabi [b], Salah Merah [b], Yahia Harek [b]

[a] *Département de Biologie, Faculté des sciences et de la technologie, Université Tahar Moulay, Saïda, Algérie*
[b] *Département de Chimie, Faculté des Sciences, Université Abou Bakr Belkaïd, Tlemcen, Algérie*

Abstract

The inhibition effect of methylene blue dye (MBD) on the corrosion of mild steel in 0.5 M sulphuric acid solution at 30°C was studied by weight loss, potentiodynamic polarization and electrochemical impedance spectroscopy (EIS) methods. The results show that MBD is an excellent inhibitor even with very low concentration, and the adsorption of methylene blue dye (MBD) on the mild steel surface obeys Langmuir adsorption isotherm. Potentiodynamic polarization curves reveal that MBD behaves as a mixed-type inhibitor. EIS spectra exhibit one capacitive loop and confirm the inhibitive ability. Some thermodynamic functions of dissolution and adsorption processes were also determined. The obtained results indicated that MBD is chemically adsorbed on the steel surface.

Keys words: Methylene blue dye (MBD), corrosion, inhibition, mild steel, sulphuric acid, adsorption,

1. Introduction

Sulphuric acid is widely used in various industries for the pickling of ferrous alloys and steels. Because of the aggressive nature of the acid medium, the inhibitors are commonly used to reduce acid attack on the substrate metal. Most of the reported corrosion inhibitors are organic compounds containing P, N, O and S in their structures [1-12].
However, the stability of the inhibitor film formed over the metal surface depends on some physicochemical properties of the molecule, related to its functional groups, aromaticity, the possible steric effects, elec-tronic density of donors, type of the corrosive medium and nature of the interaction between the inhibitors with the d-orbital vacant of iron [13–17]. In the other hand, organic dyes have been reported as effective corrosion inhibitors of mild steel in acidic media [18- 20]. In our previous work we have studied the synergistic effect of iodide ions in the performance of Methyl Red as a corrosion inhibitor of carbon steel in 0.5 M H_2SO_4 [21]. The present work is an extension of the earlier work and study the influence on the corrosion inhibition of mild steel in sulphuric acid solution, of methylene blue dye (MBD) which acts as a good inhibitor with steel in 1 M HCl [22] and 2M M H_2SO_4 solutions [23].
Weight loss measurements and electrochemical techniques (impedance spectroscopy, potentiodynamic polarization and polarisation resistance) were carried out to study the performance of MBD as a corrosion inhibitor of carbon steel in 0.5M H_2SO_4. Results are reported and discussed.

2. Experimental

2.1. Materials and inhibitor
The mild steel strips used have a chemical composition as follows (in %):

C	Si	S	P	Mn	Fe
0.30-0.35	0.15-0.35	0.035	0.035	0.05-0.1	balance

The methylene dye blue (Merck) was used as received. Figure1 shows the molecular structures the methylene dye blue (MBD). The acidic solution used was made of analytical grade 98% H_2SO_4. Appropriate concentration of acid was prepared using double-distilled water.
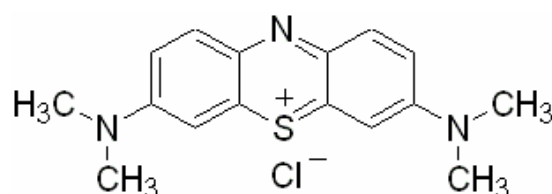

Figure 1. Molecular structure of MBD

2.2. Gravimetric measurements
The specimens for weight loss measurements were 20 mm by 10 mm by 1 mm. They were polished with emery paper (from 400 to 1000 grade). Each run was carried out in a glass vessel containing 100 ml test solution. A clean weighed mild steel specimen was completely immersed at an inclined position in the vessel.
After 2 hour of immersion in 0.5 M H_2SO_4 with and without addition of MBD at different concentrations, the specimen was withdrawn, rinsed with distilled water, washed with acetone, dried and weighed using an analytical balance accurate to 0.01 mg. The weight loss was used to calculate the corrosion rate in milligrams per square centimeter per hour.

2.3. Electrochemical measurements
Disc electrode (0.5 cm^2 area) was prepared from the investigated mild steel. The electrode was polished with emery papers (from 400 to 1000), rinsed with distilled water, degreased by acetone, washed thoroughly with bi-distilled water and dried at room temperature. The concentration range of inhibitor employed was $5x10^{-4}$ to $5x10^{-3}$M. The studies were carried out potentiodynamically in a thermostated electrolytic cell. Platinum disc was used as a counter-electrode (CE) and a saturated calomel electrode as a reference electrode (SCE). The latter was connected through a Luggin's capillary to the cell. The working electrode (WE) was immersed in a test solution for 2 h until a steady state open-circuit potential (E_{ocp}) was obtained. The potentiodynamic current-potential curves were recorded by changing the electrode potential automatically from –700 to –300 mV with scanning rate of 0.5 mV s^{-1} under static conditions using the PGZ301 potentiostat-galvanostat (VoltaLab40-Radiometer). All experiments were carried out in freshly prepared solution at constant temperatures, 25°C, 30°C, 40°C and 50°C ± 0.1 °C using a thermostat.
Electrochemical impedance spectroscopy (EIS) was conducted in an electrochemical measurement system (VoltaLab40), which comprises a PGZ301 potentiostat, a personal computer, VoltaMaster 4 and Zview software. The ac impedance measurements were performed at corrosion potentials (E_{corr}) over a frequency range of 10 kHz ₋ 20 mHz, with a signal amplitude perturbation of 10 mV. The data were plotted and analyzed using software VoltaMaster 4, version 4. The impedance parameters were calculated using software Z-View, version 2.80, 2002, Scribner Associates Inc.
The polarisation resistance measurements were performed, immediately after EIS on the same electrode without any surface treatment, by applying a controlled potential scan over a small range typically ± 15 mV with respect to E_{corr}. The resulting current is linearly plotted versus potential, the slope of this plot at E_{corr} being the polarisation resistance (R_p).

3. Results and discussion

3.1. Weight loss measurements

The gravimetric measurements of mild steel in 0.5 M H_2SO_4 in the absence and presence of various concentrations of MBD investigated were determined after 2 hour of immersion at 30°C. The inhibition efficiency of the inhibitor for the corrosion of mild steel was calculated as follows [15].

$$P\% = \frac{W - W_{inh}}{W} x100 \qquad (1)$$

where W and W_{inh} are the uninhibited and the inhibited corrosion rate, respectively.

Table 1 gives values of the corrosion rates and percentage inhibition efficiency calculated from the weight loss measurements for different concentrations of MBD. The mild steel corrosion rate decrease with increasing concentration of inhibitors. At this purpose, one observes that the optimum concentration of inhibitor required to achieve the efficiency is found to be 5×10^{-3} M (P = 81.08%).

Table 1. Corrosion rates and inhibition efficiencies of MBD at different concentrations in 0.5 M H_2SO_4

Conc. (M)	W (mg/cm^{2}h)	P (%)
Blank	0.74	-----
$5x10^{-4}$	0.23	**68.92**
$7.5x10^{-4}$	0.17	**77.02**
10^{-3}	0.16	**78.38**
$2.5x10^{-3}$	0.15	**79.73**
$5x10^{-3}$	0.14	**81.08**

3.2. Polarization curves

Both anodic and cathodic polarization curves of mild steel in 0.5 M H_2SO_4 acid at various concentrations of MBD are shown in Figure 2.

It can be seen from figure 2 that, in the presence of the inhibitor, the curves are shifted to lower current regions, showing the inhibition tendency of MBD. The values of various electrochemical parameters are summarized in table 2. The corrosion current densities were estimated by Tafel extrapolation of the cathodic curves to the open circuit corrosion potentials.

Inhibition efficiency was then calculated using the expression:

$$P\% = \frac{i_{corr}^0 - i_{corr}}{i_{corr}^0} x100 \qquad (2)$$

where I_{corr}^0 is the corrosion current density in uninhibited acid and I_{corr} is the corrosion current density in inhibited acid.
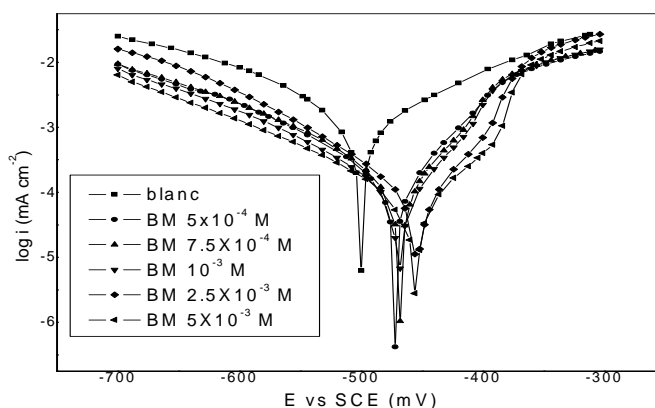

Figure 2. Polarization curves of mild steel in 0.5 M H_2SO_4 in the presence of different concentrations of MBD at 30°C.

Table 2 shows that an increase in inhibitor concentration is resulted in increased inhibition efficiency. It is evident from the results that the I_{corr} values decrease considerably in the presence of inhibitor and that the maximum decrease in I_{corr} coincides with the optimum concentration of inhibitor. The compound studied performed excellently (95% inhibition efficiency at 5×10^{-3} M) as inhibitor of the corrosion of mild steel in 0.5 M H_2SO_4. Linear polarization technique was performed in 0.5 M H_2SO_4 with various concentrations of MBD. The corresponding polarization resistance (R_p) values of mild steel in the absence and in the presence of different inhibitor concentrations are also given in table 2. It is apparent that R_p increases with increasing inhibitor concentration. The inhibition percentage (P%) calculated from R_p values are also presented in table 2. We remark that P% increases with increasing concentration of inhibitor and attains 92% at 5×10^{-3} M.

The inhibition efficiencies of MBD obtained by potentiodynamic polarization and by polarization resistance methods are in good agreement, particularly, at high concentrations.

For anodic polarization, it can be seen from Fig. 2 that, in the presence of MBD at high concentrations, two linear portions were observed. When the anodic potentials increases, the anodic current increases at a slope of b_{a1} in the low polarization potential region. After passing a certain potential E_u, the anodic current increases rapidly and dissolves at a slope of b_{a2} in the high polarization region. This behavior was already documented for iron in acid solutions [7, 24- 27].

The rapid increase of anodic current after E_u may be due to desorption of MBD molecules adsorbed on the electrode. This means that the inhibition mode of MBD depends on electrode potential. In this case, the observed inhibition phenomenon is generally described as corrosion inhibition of the interface associated with the formation of a bidimensional layer of adsorbed inhibitor species at the electrode surface [28]. Note that the potential E_u is also denoted E_1 in Bartos and Hackerman's paper [24]. Figure 2 shows also that, at potentials higher than E_{corr}, MBD affects the anodic reaction. This result indicates that MBD exhibits both anodic and cathodic inhibition effect.

Table 2: Electrochemical parameters of mild steel in 0.5 M H_2SO_4 in the absence and presence of different concentrations of MBD at 30°C.

Conc. (M)	E_{corr} *vs* SCE (mV)	i_{corr} (mA/cm)	Rp ($\Omega.cm^2$)	b_c (mV/dec°)	(P)i_{corr} (%)	(P)$_{Rp}$ (%)
Blank	-498	1.96	17	158	---	---
$5x10^{-4}$	-471	0.18	105	116	**90.81**	**83.81**
$7,5x10^{-4}$	-471	0.14	112	112	**92.85**	**84.82**
10^{-3}	-467	0.13	146	120	**93.37**	**88.36**
$2,5x10^{-3}$	-450	0.11	181	96	**94.38**	**90.60**
$5x10^{-3}$	-455	0.09	215	125	**95.40**	**92.09**

3.2. Electrochemical impedance spectroscopy (EIS)
Figure 3 shows the Nyquist diagrams for mild steel in 0.5 M H_2SO_4 at 30 °C after immersion of 2 hours containing various concentrations of MBD. The impedance spectra exhibit one single depressed semicircle, and the indicates that the charge transfer takes place at electrode/solution interface, and the transfer process controls corrosion reaction of steel and the presence of inhibitor does not change the mechanism of steel dissolution [29].

Also, these impedance diagrams are not perfect semicircles which are related to the frequency dispersion as a result of the roughness and inhomogeneous of electrode surface [30]. Furthermore, it is apparent, from these plots that, the impedance response of mild steel in uninhibited H_2SO_4 solution has significantly changed after addition of MBD in the corrosive solution; as a result, real axis intercept at high and low frequencies in the presence of inhibitor is bigger than that in the absence of inhibitor (blank solution) and increases as the inhibitor concentration increases. This confirms that the impedance of inhibited substrate increases with the concentration of MBD in 0.5 M H_2SO_4.

The EIS results are simulated by the equivalent circuit shown in figure 4 to pure electric models that could verify or rule out mechanistic models and enable the calculation of numerical values corresponding to the physical and/or chemical properties of the electrochemical system under investigation [31].
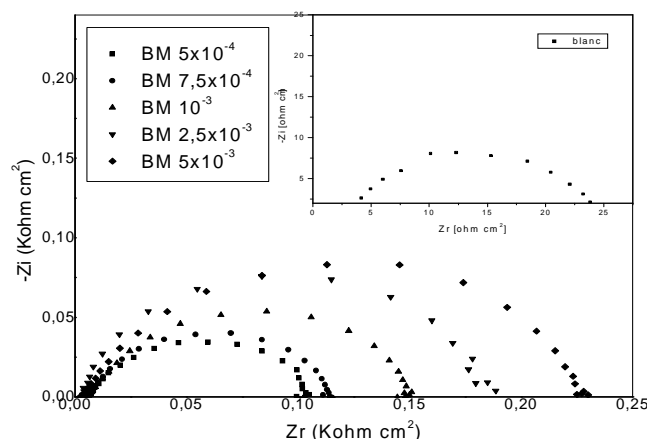
Figure 3. Nyquist plot of mild steel in aerated 0.5 M H_2SO_4 acid solution at different concentrations of MBD after 2 hours.
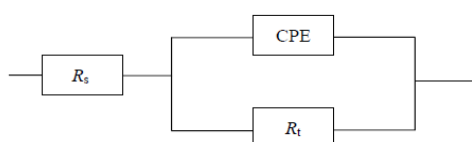

Figure 4. Equivalent circuit used to fit the EIS data of mild steel in 0.5 M H_2SO_4 without and with different concentrations of MBD

The circuit employed allows the identification of both solution resistance (R_s) and charge transfer resistance (R_t). It is worth mentioning that the double layer capacitance (C_{dl}) value is affected by imperfections of the surface, and that this effect is simulated via a onstant phase element (CPE) [32]. The constant phase element is composed of a component Q_{dl} and a coefficient n. The parameter n quantifies different physical phenomena like surface inhomogeneousness resulting from surface roughness, inhibitor adsorption, porous layer formation, etc. So the capacitance is deduced from the following relation [33]:

$$C_{dl} = Q_{dl} x \left(2\pi f_{max}\right)^{n-1} \tag{3}$$

where f_{max} represents the frequency at which imaginary value reaches a maximum on the Nyquist plot. The electrochemical parameters are summarized in Table 3.

The inhibition efficiency is calculated by charge transfer resistance as follows [34:

$$P\% = \frac{R_t - R_t^0}{R_t} x 100 \tag{4}$$

where R_t^0 and R_t are the charge transfer resistance values without and with inhibitor for mild steel in acidic media, respectively.

Table 3. EIS parameters for the corrosion of mild steel in 0.5 M H_2SO_4 containing MBD at 30 ^{o}C after 2 hours of immersion

Conc. (M)	$Q(S^n/\Omega cm^2)$	n	R_t ($\Omega.cm^2$)	C_{dl} ($\mu F/cm^{-2}$)	P (%)
Blank	12.0 x10^{-4}	0.81	21.67	547	**----**
5x10^{-4}	3.80 x10^{-4}	0 .76	101.05	158	**82.22**
7.5x10^{-4}	4.00 x10^{-4}	0.79	110.70	174	**83.77**
10^{-3}	3.60 x10^{-4}	0.75	148.10	146	**87.90**
2.5x10^{-3}	1.99 x10^{-4}	0.90	180.05	137	**90.06**
5x10^{-3}	2.60 x10^{-4}	0.77	229	111	**92.16**

As shown in Table 3, R_t values increases prominently while C_{dl} reduces with the concentration of MBD. The decrease in C_{dl} comparing with that in blank solution (without inhibitor), which can result from a decrease in local dielectric constant and/or an increase in the thickness of the electrical double layer, suggests that the inhibitor molecules function by adsorption at the metal/solution interface [35]. P% increases with the concentration of MBD, and the maximum P% reaches up to 92.2%, which further confirm MBD exhibits good inhibitive performance for mild steel in 0.5 M H_2SO_4.

Inhibition efficiencies obtained from potentiodynamic polarization curves and EIS are in good reasonably agreement.

3.4 . The adsorption isotherm

Assuming the increase of the inhibition is caused by the adsorption of inhibitor on the CRS surface and obeys Langmuir adsorption isothermal equation [10, 36, 38]

$$\frac{C}{\theta} = \frac{1}{K} + C \qquad (5)$$

where C is the concentration of inhibitor, K the adsorptive equilibrium constant and θ is the surface coverage and calculated by the following equation [10, 36, 38]:

$$\theta = \frac{i^0_{corr} - i_{corr}}{i^0_{corr}} x100 \qquad (6)$$

where i^0_{corr} is the corrosion current density in uninhibited acid and i_{corr} is the corrosion current density in inhibited acid.

Plotting C/θ versus c yields a straight line as shown in Figure 5. The linear correlation coefficient (r) is almost equal to 1 ($r = 0.9999$) and the slope is very close to 1 (slope = 1.04), indicating the adsorption of MBD on steel surface obeys Langmuir adsorption isotherm. The adsorptive equilibrium constant (K) value is 3.75×10^4 L/mol.
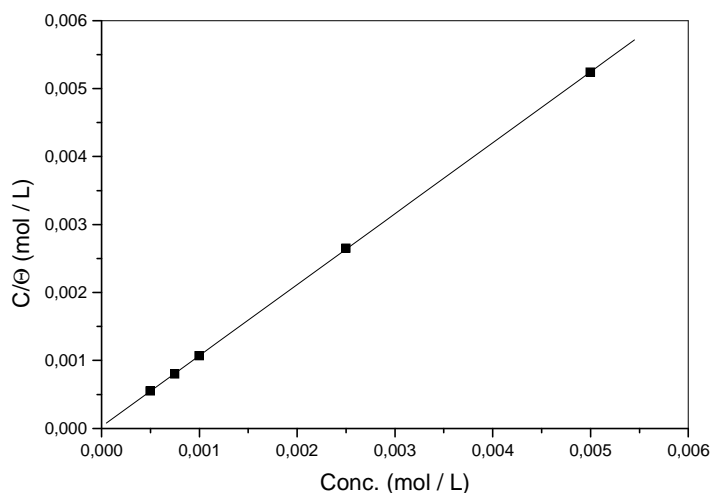

Figure 5. The relationship between C/θ and C in 0.5 M H_2SO_4.

It is related to the standard free energy of adsorption (ΔG_{ads}) as shown the following equation [11-12, 14]:

$$K = \frac{1}{55.5} \exp(\frac{-\Delta G_{ads}}{RT}) \qquad (7)$$

where R is the gas constant (8.314 J / K.mol), T the absolute temperature (K), the value 55.5 is the concentration of water in solution expressed in M [37-38].

The ΔG_{ads} value calculated is -36.65 kJ/mol. The negative values of ΔG_{ads} indicate that the adsorption of inhibitor molecule onto steel surface is a spontaneous process. Generally, values of ΔG_{ads} up to -20 kJ/mol are consistent with the electrostatic interaction between the charged molecules and the charged metal

(physical adsorption) while those more negative than -40 kJ/mol involve sharing or transfer of electrons from the inhibitor molecules to the metal surface to form a co-ordinate type of bond (chemisorption) [1, 21, 39-41] In the present study, the value of ΔG_{ads} is about equal to -40 kJ/mol; probably mean that the adsorption mechanism of the MBD on steel in 0.5 M H_2SO_4 solution is mainly the chemisorption. Noticeably, it is generally accepted that physical adsorption is preceding stage of chemisorption of inhibitors on metal surface [42].

The adsorption process is affected by the chemical structures of the inhibitors, the nature and charged surface of the metal and the distribution of charge over the whole inhibitor molecule. In general, owing to the complex nature of adsorption and inhibition of a given inhibitor, it is impossible for single adsorption mode between inhibitor and metal surface. In the present system, based on the chemical structure of MBD, MBD has many active sites for the adsorption process. Acoording Xianghong Li at al [38], five types of adsorption may take place in the inhibiting phenomena involving BT molecules on steel surface as follows:

- MBD can be classified as an electrolyte, namely, the organic part (MBD^+) is the cation and the inorganic part (Cl^-) is the anion:
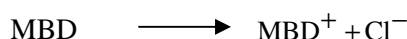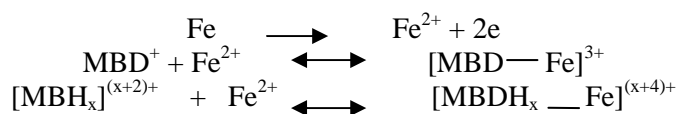
$$MBD \longrightarrow MBD^+ + Cl^-$$

Owing to neutral N atoms in MBD^+, MBD^+ could further be protonated in the acid solution as following:

$$MDB^+ + xH^+ \longleftrightarrow [MBH_x]^{(x+2)+}$$
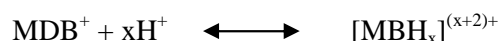
Thus, in aqueous acidic solutions, the BT exists as protonated cations of MBD^+ and $[MBDH_x]^{(x+2)+}$. Since chloride (Cl^-) and sulphate (SO_4^{2-}) ions have a smaller degree of hydration, being specifically adsorbed, they create an excess negative charge towards the solution and favour more adsorption of the cations [38, 43] MBD^+ and $[MBDH_x]^{(x+2)+}$ may adsorb on the negatively charged metal surface, namely, i.e. there may be a synergism between these ions and protonated MBD.

- It should be noted that the molecular structure of MBD^+ and $[MBDH_x]^{(x+2)+}$ remains unchanged with respect to MBD, that is, the N and S atoms on the ring remaining strongly blocked, MBD^+ and $[MBDH_x]^{(x+2)+}$ may be adsorbed on the metal surface via the chemisorption mechanism, involving the displacement of water molecules from the metal surface and the sharing electrons between the N atoms and iron [11] .

- Because MBD contains aromatic rings with several π bonds, MBD^+ and $[MBDH_x]^{(x+2)+}$ molecules can be also adsorbed on the metal surface on the basis of donor-acceptor interactions between π-electrons of the heterocycles and vacant d-orbitals of Fe. The larger molecule area plays an important role in retarding the corrosion [10-12].

- MBD^+ and $[MBDH_x]^{(x+2)+}$ may combine with freshly generated Fe^{2+} ions on steel surface forming metal inhibitor complexes:

$$Fe \longrightarrow Fe^{2+} + 2e$$
$$MBD^+ + Fe^{2+} \longleftrightarrow [MBD-Fe]^{3+}$$
$$[MBH_x]^{(x+2)+} + Fe^{2+} \longleftrightarrow [MBDH_x \underline{\ \ } Fe]^{(x+4)+}$$

These complexes might adsorb onto steel surface by the van der Waals force to form a blocking barrier to keep mild steel from corrosion.

- A combination of the above.

3.4. Effect of temperature

To investigate the mechanism of inhibition and to determine the activation energy of the corrosion process, polarization curves of steel in 0.5 M H_2SO_4 were determined at various temperatures (303–333 K) in the absence and presence of $5x10^{-3}$ M of MBD.

Figure 6 presents the Arrhenius plots of the natural logarithm of the current density *vs* 1/T, for 0.5 M solution of sulphuric acid, without and with addition of MBD. Straight lines with coefficients of correlation (c.c.) high to 0.99 are obtained for the supporting electrolyte and MMI.

The values of the slopes of these straight lines permit the calculation of the Arrhenius activation energy, E_A^*, according to :

$$\log i_{corr} = \frac{E_A^*}{RT} - \log A \tag{8}$$

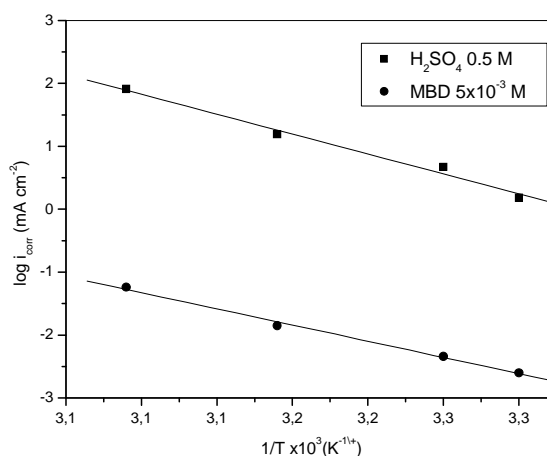where R is the universal gas constant and A is the Arrhenius factor.

Figure 6. Arrhenius plots of log i_{corr} versus 1/T without an with 5×10^{-3}M of MBD

The calculated values of E_A^* are 52.54 kJ/mol (blank) and 42.73 kJ/mol (MBD). The value of E_A in the presence of MBD is low as compared to the uninhibited system. We remark that the addition of inhibitor modified the values of E_A ; this modification may be attributed to the change in the mechanism of the corrosion process in the presence of adsorbed inhibitor molecules [1, 44]. The lower value of the activation energy of the process in an inhibitors presence when compared to that in its absence is attributed to its chemisorption, while the opposite is the case with physical adsorption [45, 46]. The lower value of the E_A was attributed by Hoar and Holliday [47] to a slow rate of inhibitor adsorption with a resultant closer approach to equilibrium during the experiments at the higher temperature. But, Riggs and Hurd [48] explained that the decrease in activation energy of corrosion at higher levels of inhibition arises from a shift of the net corrosion reaction from that on the uncovered part on the metal surface to the covered one. Schmid and Huang [49] found that organic molecules inhibit both the anodic and cathodic partial reactions on the electrode surface and a parallel reaction takes place on the covered area, but that the reaction rate on the covered area is substantially less than on the uncovered area.

4. Conclusion

The inhibiting effect of MBD increases with increase of inhibitor concentration. Its presence in the solution decreases the value of the apparent activation corrosion energy. The adsorption of MBD on the steel surface in sulphuric acid obeys the Langmuir adsorption isotherm model and leads to the formation of a protective film.
The analysis of the experimental data leads to the suggestion of chemisorption of the inhibitor on the metal surface. In fact, the apparent activation energy of the corrosion that is lower in presence of MBD than in its absence and the higher values of the free energy of adsorption verify the chemisorptive character of the adsorption. The substance is adsorbed with the heteroatoms forming donor–acceptor bonds between unpaired electrons of the heteroatoms and the active centres of the metal surface.

References
1. Bouklah, M., Hammouti, B., Lagrenée, M., Bentiss, F., *Corros. Sci.,* 48 (2006) 2831.
2. Bouklah, M., Hammouti, B., Aouniti, A., Benhadda, T., *Prog. Org. Coat.,* 47 (2004) 225.
3. Bouzidi, D., Kertit, S., Hammouti, B., Brighli, M., *J. Electrochem. Soc. Ind.,* 46 (1997) 23.
4. Touhami, F., Aouniti, A., Kertit, S., Abed, Y., Hammouti, B., Ramdani, A., El-Kacemi, K., *Corros. Sci.,* 42 (2000) 929.
5. Kertit, S., Essouffi, H., Hammouti, B., M. Benkaddour, B., *J. Chim. Phys.*, 95 (1998) 2072.

6. Kertit, S., Bekkouche, K., Hammouti, B., *Rev. Métall.: Paris*, 97 (1998) 251.

7. F. Chaouket, B. Hammouti, S. Kertit, K. Elkacemi, Bull. Electrochem., 17 (2001) 311.

8. Singh, A. K., Quraishi., M. A. *J. Mater. Environ. Sci.,* 1 (2) (2010) 101.

9. El Ouali, I., Hammouti, B., Aouniti, A., Ramli, Y., Azougagh, M., Essassi, E.M., Bouachrine, M., *J. Mater. Environ. Sci.,* 1(1) (2010) 1.

10. Larabi, L., Harek, Y., Benali, O., ghalem, S., *Prog. Org. Coat.*, 54 (2005) 256.

11. Benali, O., Larabi, L., Tabti, B., Harek, Y., *Anti-Corros. Meth. Mat.*, 52 (2005) 280.

12. Benali, O., Larabi, L., Mekelleche, S. M., B., Harek, Y., *J. Mat. Sci.*, 41 (2006) 7064.

13. Larabi, L., Benali, O., Harek, Y., *Mat. Lett.*, 61 (2007) 3287.

14. Benali, O., Larabi, L., Traisnel, M., Gengembre, L., Harek, Y., *Appl. Surf. Sci.*, 253 (2007) 6130.

15. Roque, J. M., Pandiyan, T., Cruz, J., Garcia-Ochoa, E., *Corr. Sci.*, 50 (2008) 614.

16. D.A. Jones, *Principles and Prevention of Corrosion*, second ed., Prentice-Hall Inc., New Jersey, 1996.

17. V.S. Sastry, *Corrosion Inhibitors. Principles and Applications*, John Wiley & Sons, New York, 1998.

18. Ebenso, E.E., Oguzie, E.E., *Mater. Lett.*, 59(17) (2005) 2163.

19. Tirbonod, F., Fiaud, C., *Corros. Sci.*, 18 (1978) 139.

20. Ebenso, E.E., *Bull. Electrochem.*, 19 (5) (2003) 209.

21. Merah, S., Larabi, L., Benali, O., Harek, Y., *Pigm. Res. Tech.*, 37 (5) (2008) 291.

22. Oguzie, E.E., *Mater. Lett.*, 59 (8/9) (2005) 1076.

23. Oguzie, E.E., Onnohu, G.N., Onuchukwu, A.I., *Mater. Chem. Phys.,* 89 (2005) 305.

24. Bartos, M., Hackerman, N., *J. Electrochem. Soc.*, 139 (1992) 3428.

25. Kuo, H. C., Nobe, K. J., *J. Electrochem. Soc.*, 125 (1978) 853.

26. Mac Farlane, D. R., Smedley S. I., *J. Electrochem. Soc.*, 133 (1986) 2240.

27. Feng, Y., Siow, K. S., Teo, W. K., Hseieh, A. K., *Corros. Sci.*, 41 (1999) 829.

28. Lorentz, W. J., Mansfeld, F., *Corros. Sci.,* 31 (1986) 467.

29. Larabi, L., Harek, Y., Traisnel, M., Mansri, A., *J. Appl. Electrochem.*, 34 (2004) 833.

30. Lebrini, M., Lagrenée, M., Vezin, H., Traisnel, M., Bentiss, F., *Corros. Sci.,* 49 (2007) 2254.

31. Priya, A.R.S., Muralidharam, V.S., Subramanian, A., *Corrosion*, 64 (2008) 541.

32. Bommersbach, P., Alemany-Dumont, C., Millet, J.P., Normand, B*., Electrochim. Acta*, 51 (2006) 4011.

33. Qu, Q., Hao, Z.Z., Li, L., Bai, W., Liu, Y.J., Ding, Z.T., *Corros. Sci.*, 51 (2009) 569.

34. Kissi, M., Bouklah, M., Hammouti, B., Benkaddour, M., *Appl. Surf. Sci.*, 252 (2006) 4190.

35. Lagrenée, M., Mernari, B., Bouanis, M., Traisnel, M., Bentiss, F., *Corros. Sci.,* 44 (2002) 573.

36. Tsuru, T., Haruyama, S., Gijutsu, B., *J. Jpn. Soc. Corros. Eng.,* 27 (1978) 573.

37. Cano, E., Polo, J.L., La Iglesia, A., Bastidas, J.M., *Adsorption*, 10 (2004) 219.

38. Xianghong Li, Shuduan Deng, Hui Fu, *Corros. Sci.,* 52 (2010) 2786.

39. Wang, H.L., Fan, H.B., Zheng, J.S., *Mater. Chem. Phys.,* 77(3) (2002) 655.
40. Donahue, F.M., Nobe, K., *J. Electrochem. Soc.*, 112(9) (1965) 886.
41. Metikosˇ-Hukovic, M., Babic, R., Grubac´, Z., Brinic, S., *J. Appl. Electrochem.*, 26 (1996) 443.
42. Wang, F.P., Kang, W.L., Jin, H.M., *Corrosion Electrochemistry Mechanism, Methods and Applications*, Chemical Industrial Engineering Press, Beijing, 2008, p. 242.
43. Bentiss, F., Traisnel, M., Lagrenée, M., *Corros. Sci.*, 42 (2000) 127.
44. B. Mernari, L. Elkadi, S. Kertit, *Bull. Electrochem.*, 17 (2001) 115.
45. Szauer, T., Brandt, A., *Electrochim. Acta*, 26 (1981) 1209.
46. Dahmani, M., Et-Touhami, A., Al-Deyab, S.S., Hammouti, B., Bouyanzer, A. *Inter. J. Electrochem. Sci.* 5 (2010) 1060.
47. Hoar, T.P., Holliday, R.D., *J. Appl. Chem.*, 3 (1953) 502.
48. Riggs Jr., O.L., Hurd, R.M., *Corrosion*, 23 (1967) 252.
49. Schmid, G.M., Huang, H.J., *Corros. Sci.,* 20 (1980) 1041.